

Dinuclear Ru(II) dyes for improved performance of dye-sensitized TiO₂ solar cells

Youngju Lee, Song-Rim Jang, R. Vittal and Kang-Jin Kim*

Received (in Durham, UK) 14th May 2007, Accepted 8th August 2007

First published as an Advance Article on the web 20th August 2007

DOI: 10.1039/b707220a

In this study, a Ru(II) dye was linked to another TiO₂-attached Ru(II) dye through the linker, *trans*-1,2-bis(4-pyridyl)ethylene (*tbpe*), and such TiO₂ film electrodes were used in dye-sensitized solar cells (DSSCs). The mononuclear Ru(II) dyes selected were N3 ([Ru(dcbpyH₂)₂(NCS)₂], dcbpyH₂ = 2,2'-bipyridyl-4,4'-dicarboxylic acid), N719 ([Ru(dcbpyH₂)(NCS)₂]), and N749 ([Ru(tcterpy)(NCS)₃]·3H₂O, tcterpy = 4,4',4''-tricarboxy-2,2':6',2''-terpyridine). The photovoltaic characteristics of the DSSCs prepared using the above-mentioned TiO₂ film electrodes were examined. The DSSC with the dinuclear dye, N719-*tbpe*-N719 had the highest short-circuit photocurrent density (*J*_{sc}) and thereby the highest conversion efficiency compared with the other cells sensitized by the other mononuclear or dinuclear Ru(II) dyes. The *J*_{sc} enhancement was attributed to an increase in the conduction band electrons of TiO₂ due to the efficient intramolecular charge and energy transfer from the linked dye molecule to the immobilized molecule through a chain of conjugated double bonds in *tbpe*. These transfers are explained based on the relative LUMO levels of the dyes.

Introduction

Several mononuclear Ru(II) dyes, such as N3 ([Ru(dcbpyH₂)₂(NCS)₂], where dcbpyH₂ = 2,2'-bipyridyl-4,4'-dicarboxylic acid), N712 ([Ru(dcbpyH₂)₂(NCS)₂]), N719 ([Ru(dcbpyH₂)(NCS)₂]), and N749 ([Ru(tcterpy)(NCS)₃]·3H₂O, where tcterpy = 4,4',4''-tricarboxy-2,2':6',2''-terpyridine), have been used as efficient sensitizers in DSSCs.^{1–4} Considerable efforts have been made to improve the cell performance using the N3 dye by attaching hydrophobic chains to the pyridine rings of N3^{5,6} (to increase the open circuit voltage), substituting NCS ligands with other ligands⁷ (for panchromatic sensitization of TiO₂), and finding analogues to Ru(II)-based sensitizers with metal centers such as Re,⁸ Rh,⁹ and Os,¹⁰ *i.e.*, the analogues [(4,4'-(CO₂H)₂bpy)Re^I(CO)₃-CN-Ru^{II}(bpy)₂(CN)](PF₆),⁸ Rh^{III}(4,4'-dicarboxy-2,2'-bpy)₂-(1,2-bis{4-(4'-methyl-2,2'-bipyridyl)}ethane)-Ru^{II}(4,7-dimethyl-1,10-phenanthroline)₂,⁹ and [Ru{4,4'-(CO₂H)₂-2,2'-bpy}₂(Cl)-1,2-bis(4-pyridyl)-ethane-Os(bpy)₂(Cl)]-(PF₆)₂,¹⁰ respectively. Recently Islam *et al.* reported the very efficient panchromatic sensitization of TiO₂ over the whole visible range extending into the near IR region of approximately 950 nm through a ruthenium(II) tricarboxyterpyridyl complex with a fluorine-substituted β-diketonato ligand,¹¹ *i.e.*, the complex Ru(4,4',4''-tricarboxy-2,2':6',2''-terpyridine)[4,4,4-trifluoro-1-(4-fluorophenyl)-butane-1,3-dionato](NCS)[(C₄H₉)₄N]₂. In addition to organometallic dyes, organic dyes have also been used as sensitizers in DSSCs on account of their low production cost, which is attributable to their simple molecular structures and

synthetic procedures.¹² Thus far, the newly developed dyes could not significantly improve the efficiency of a DSSC achieved with a mononuclear Ru(II) dye. The search for new efficient dyes is ongoing.

Lees *et al.* examined the photophysical properties of the dinuclear complexes Ru(II)-bpt-Ru(II) and Ru(II)-bpt-Os(II) (bpt = 3,5-bis(pyridin-2-yl)-1,2,4-triazole), and reported that the incident-photon-to-current-conversion efficiency (IPCE) in the case of Ru(II)-bpt-Ru(II) was approximately half that obtained for the cell prepared using the mononuclear Ru(II) compound.¹³ This greatly reduced IPCE might be due to the lower level of adsorption of the dinuclear complex onto the TiO₂ surface, compared with that of the Ru(II) complex. Furthermore, a regenerative solar cell with Ru(II)-bpt-Os(II) produced virtually no photocurrent.¹⁰ A DSSC made using a rod-like homometallic dinuclear Ru(II) complex linked by 4'-(4-methylphenyl)-2,2':6',2''2,2'-terpyridine showed an overall conversion efficiency of only 1.9%.¹⁴ Recently, we reported a new *in situ* route for the attachment of N3, using *trans*-1,2-bis(4-pyridyl)ethylene (*tbpe*), to another N3, which was already immobilized onto nanocrystalline TiO₂. The *J*_{sc} of the cell with this N3-*tbpe*-N3 dinuclear complex was significantly higher than the *J*_{sc} of a DSSC with N3.¹⁵ The linker *tbpe* connects the two Ru(II) metal centers of the dinuclear complex by a chain of conjugated double bonds, which facilitates electron transfer from the linked N3 to the immobilized N3. The photophysical behavior of heterometallic dinuclear Rh-Ru complexes, bridged by 1,2-bis-[4-(4'-methyl-2,2'-bipyridyl)]ethane, was investigated in terms of the stepwise charge separation. However, only a small photocurrent was obtained in this case due to the weak light absorption.⁹ Loiseau *et al.* reported the funneling of light absorbed by four Ru(bpy)₃²⁺-type chromophores to another Ru(bpy)(CN)₄²⁻ subunit.¹⁶

Department of Chemistry, Korea University, Seoul 136-713, Korea.
E-mail: kjkim@korea.ac.kr; Fax: +82 2 3290 3121;
Tel: +82 2 3290 3127

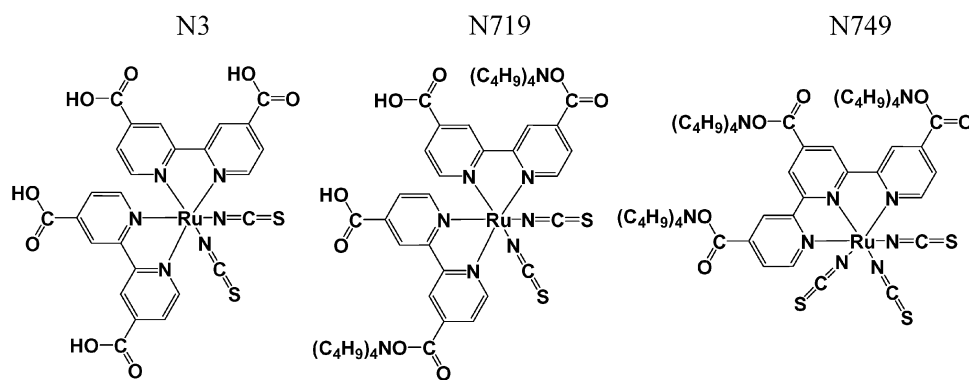


Fig. 1 Molecular structures of N3, N719 and N749.

There were reports on the photophysical properties of dimetallic complexes, such as polymeric system with $\text{Ru}_{17}\text{Os}_3$,¹⁷ the complex $[\text{Ru}(\text{bpy})_3(\text{ph})_n\text{Os}(\text{bpy})_3]^{4+}$,¹⁸ where $\text{ph} = 1,4\text{-phenylene}$ and $n = 3, 5, 7$, and the complex $(\text{bpy})_2\text{Os}(\text{bpy-S-bpy})\text{Os}(\text{bpy})_2^{4+}$,¹⁹ where S is a spacer, of trimetallic complex,²⁰ $[(\text{bpy})_2\text{Ru}(\text{dpp})]_2\text{RhCl}_2(\text{PF}_6)_5$, and of supramolecular complexes, *e.g.*, $[(\text{bpy})_2\text{Os}(\text{bpy-An-bpy})\text{Os}(\text{bpy})_2]^{4+}$,²¹ where An is anthracene, or $[\text{Ru}(\text{Pyr}_n\text{bpy})(\text{CN})_4]^{2-}$ ($n = 1, 2$)²² or $[\text{Ru}(\text{H1})(\text{bpy})_2]^{2+}$ (H1 is 1-(4-carboxyphenyl)-3-(2-pyridyl)-4,5,6,7-tetrahydroindazole).²³ However, the focus of these reports was not on DSSCs. There is only one report¹⁴ that focused on the photovoltaic properties of DSSCs using mono- (*m*-RuTerbp) and dinuclear (*d*-RuTerbp) ruthenium complexes containing terpyridine and bipyridine ligands. They reported an overall conversion efficiency of 1.9% for the cell with *d*-RuTerbp, compared with 1.1% and 4.7% for the cells with *m*-RuTerbp and N3, respectively. We believe that an overall conversion efficiency of 5.8% for a cell with the dinuclear complex N719-*tbpe*-N719 is significant, especially since this study did not focus on further optimization of the efficiency of the cell. The present paper reports the photovoltaic performance of the DSSCs sensitized by various Ru(II)-*tbpe*-Ru(II) dinuclear complexes *versus* the performance of the cells sensitized only by Ru(II) mononuclear complexes. The Ru(II) complexes used are N3, N719, and N749. Fig. 1 shows their molecular structures.

Results and discussion

Characterization of the dinuclear Ru(II) dyes

Since a Ru(II) dye-coated TiO_2 film was immersed in an ethanol solution containing a large excess of *trans*-1,2-bis(4-pyridyl)ethylene (*tbpe*) (see Experimental), most of the dye molecules on the TiO_2 particles were expected to be covalently attached to *tbpe* through the formation of a Ru–N bond due to the replacement of an NCS ligand of the dye with a *tbpe* molecule. This process leads to the formation of *tbpe*-Ru(II)- TiO_2 .²⁴ However, in the subsequent process of linking another Ru(II) dye to *tbpe*-Ru(II)- TiO_2 , not all of the TiO_2 -attached *tbpe*-Ru(II) complexes were expected to be linked to the new Ru(II) dye at the other end of the linker. Fig. 2 shows a schematic diagram of a TiO_2 particle coated with the complex, N719-*tbpe*-N719. The Ru(II)-*tbpe*-Ru(II) dinuclear dye on

the TiO_2 surface could be easily desorbed into an aqueous 10 mM KOH solution. The resulting KOH solution containing the dye species was passed through a Sephadex™ LH-20 column for exclusion chromatography, eluted with a 1 : 1 mixture of ethanol and methanol. Two colored bands were observed in the column during the separation, indicating the presence of two types of dye-containing species on the surface of the TiO_2 particles, which were verified to be Ru(II)-*tbpe*-Ru(II) and Ru(II)-*tbpe* by UV-Vis absorption spectra (Fig. 3).

Fig. 3 shows the UV-Vis absorption spectra of N719, N719-*tbpe*, and N719-*tbpe*-N719 in the 1 : 1 ethanol and methanol solution. In this case, where both the immobilized and linked dye is N719, the absorption spectrum of N719-*tbpe*-N719 shows a blue shift with respect to the spectrum of the mononuclear N719. This blue shift is consistent with the results obtained when the NCS ligands of N3 were replaced by one or two 4-phenylpyridine ligands.^{15,24} We have previously established the linkage of N3 to N3 by FTIR, where the linkage occurred at the NCS ligands of the two complexes through *tbpe*. The linkage between the two N719 complexes in Fig. 2 is also shown in the same way.

UV-Vis absorption spectra were also obtained to estimate the amount of sensitizers adsorbed on the TiO_2 films (Fig. 4). Fig. 4a shows the absorption spectra of the mononuclear Ru(II) dyes in ethanol (5×10^{-5} M) as a reference (ethanol solution spectra), which shows that the molar absorptivities of N719 are higher than those of N3 over the entire visible spectral region. On the other hand, N749 shows higher molar absorptivities than N719 and N3 in the longer wavelength

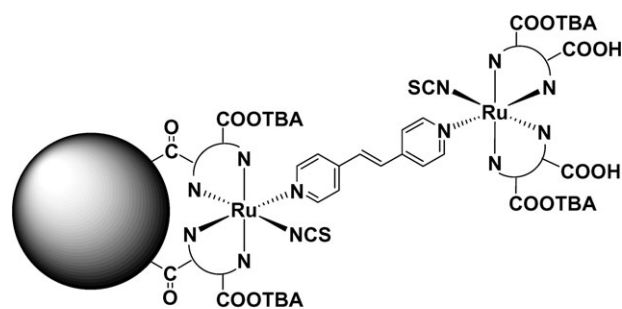


Fig. 2 Schematic diagram of a TiO_2 particle coated with the N719-*tbpe*-N719 complex.

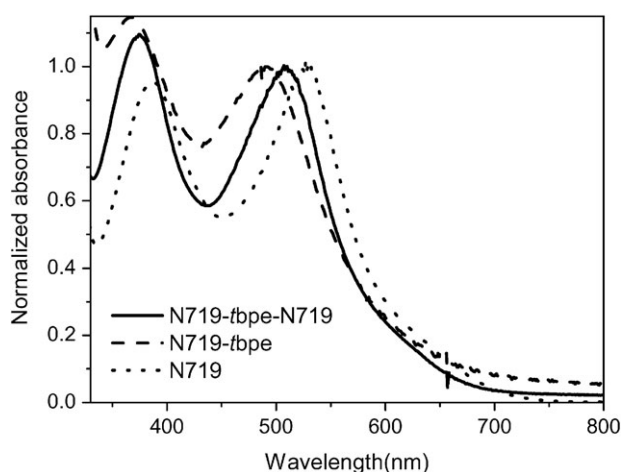


Fig. 3 UV-Vis spectra of N719, N719-*tbpe* and N719-*tbpe*-N719. The latter two were separated by exclusion chromatography using a 1 : 1 solvent of ethanol and methanol.

region. Fig. 4b (film spectra) shows the absorption spectra of N719-TiO₂ and N719-*tbpe*-Ru(II)-TiO₂ films, each with an area of 1.0 cm × 1.0 cm and thickness of 13 μm, in which Ru(II) is N3, N719 or N749. Fig. 4c (KOH solution spectra) shows the absorption spectra of the same sensitizers in Fig. 4b after they were desorbed from their corresponding TiO₂ films into 3.5 mL of aqueous 10 mM KOH. The bands at 490 and 505 nm shown in Fig. 4b and c, respectively, reveal that the absorbance ratio of each of N719-*tbpe*-Ru(II) to N719 in the respective solution spectra (Fig. 4c) is similar to their corresponding ratio in the film spectra with the background absorptions being corrected. This suggests that desorption of the N719-*tbpe*-Ru(II) sensitizers is as good as that of N719 into the corresponding KOH solutions. Fig. 4c shows a 64% increase in the absorbance of the sensitizer from the N719-*tbpe*-N719-TiO₂ film, compared with that of the sensi-

tizer from the N719-TiO₂ film. These absorption results imply that almost two thirds of the immobilized N719 molecules are linked by N719 dye molecules, in accordance with the report that the molar absorptivities of the binuclear complexes are approximately double those of the respective monomeric complexes.²⁵ The increased dye uptake in each case of the Ru(II)-*tbpe*-Ru(II)-TiO₂ film relative to that of the N719-TiO₂ film observed in Fig. 4c is attributed to the dye gained by the dinuclear complex from the linked dye. Considering the higher molar absorptivity of N719 ($1.7 \times 10^4 \text{ M}^{-1} \text{ cm}^{-1}$ at 531 nm) than those of N3 ($1.4 \times 10^4 \text{ M}^{-1} \text{ cm}^{-1}$ at 538 nm) and N749 ($0.8 \times 10^4 \text{ M}^{-1} \text{ cm}^{-1}$ at 531 nm) (Fig. 4a) as well as the corresponding increase in absorption in Fig. 4b and c, it is possible that the amount of N3 and N749 linked to their corresponding immobilized N719s are almost the same as that of the N719 linked to its immobilized N719 in terms of the number of attached molecules.

*J*_{sc} behavior of DSSCs

Fig. 5 shows the *J*-*V* curves of the DSSCs with N719-TiO₂ or Ru(II)-*tbpe*-N719-TiO₂, where Ru(II) is N3, N719 or N749. Table 1 gives a summary of the corresponding photovoltaic parameters. The table shows that the best efficiency was obtained for a DSSC fabricated using the N719-*tbpe*-N719-TiO₂ film. The *J*_{sc} of this DSSC increased to 14.3 mA cm⁻² from 10.5 mA cm⁻², the latter being the value of the cell prepared using the N719-TiO₂ film. The highest conversion efficiency for the DSSCs with the N719 dye and its dinuclear version N719-*tbpe*-N719 in this case is not surprising considering the fact that the highest efficiency obtained for any DSSC thus far was with N719.²⁶

The increase in *J*_{sc} for the DSSC with the N719-*tbpe*-N719 might be due not only to the approximate 64% increase in the amount of this dinuclear sensitizer compared with the amount of N719 (Fig. 4c), but also to the efficient intramolecular

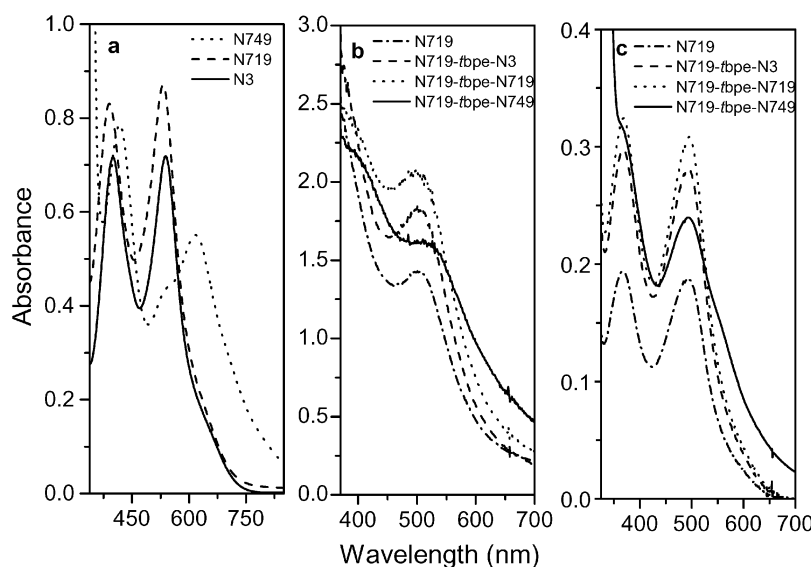


Fig. 4 UV-Vis spectra of (a) $5 \times 10^{-6} \text{ M}$ each of N719, N3, and N749 in ethanol, (b) 13 μm thick TiO₂ films coated with N719, N719-*tbpe*-N3, N719-*tbpe*-N719, and N719-*tbpe*-N749, and (c) N719, N719-*tbpe*-N3, N719-*tbpe*-N719, and N719-*tbpe*-N749 desorbed from their corresponding TiO₂ films into aqueous KOH for 3 d.

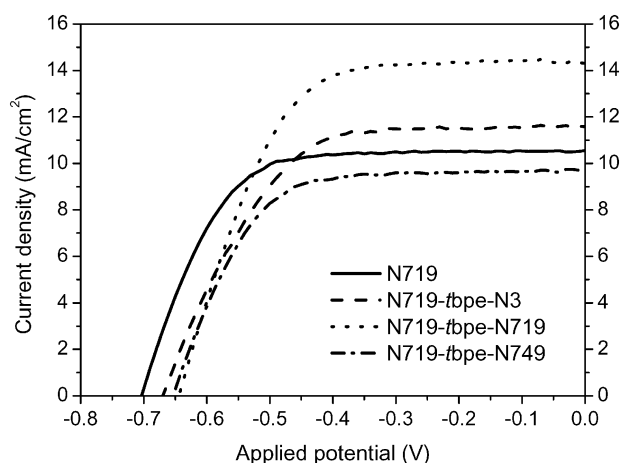
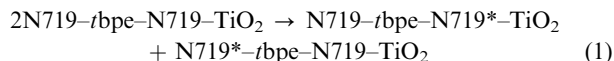
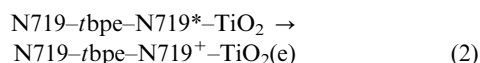


Fig. 5 J - V curves of the DSSCs prepared using the films of N719-TiO₂ and Ru(II)-*tpbe*-N719-TiO₂, in which Ru(II) is N3, N719 or N749. Light intensity was 100 mW cm⁻².

charge and energy transfer from the linked N719 to the immobilized N719. In this study, the stepwise charge injection process might be explained as follows. Excitation of N719-*tpbe*-N719-TiO₂ can lead to two different intermediate products,¹³ as shown in the reaction (1).

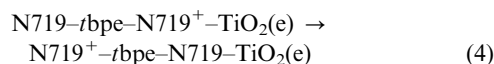


The first intermediate product injects an electron into the conduction band of TiO₂ as shown in the reaction (2) below with unit quantum yield.² With an ultrafast time constant of 50 ± 25 fs,²⁷ the electron transfer from the immobilized N719 to the conduction band of TiO₂ is expected to occur more rapidly than the vibrational relaxation within the linked N719 molecule.²⁸ The average lifetime of a vibrationally excited molecule is 10^{-12} s or less.²⁹ These time factors suggest that an electron from any excitation level of immobilized N719 moves directly to an equilevel of the conduction band of TiO₂. The second intermediate product of the reaction (1) can be converted to the first one within the nanosecond range through the energy transfer reaction (3).¹³ The resulting product rapidly injects an electron into TiO₂ according to the reaction (2). Reaction (3) suggests a process for enhancing the photocurrent for the DSSC with the N719-*tpbe*-N719-TiO₂ film, relative to that of the cell with the N719-TiO₂ film.



However, the reaction (3) has to compete with the vibrational relaxation processes within the immobilized N719. This is probably the reason for why there was only a 36% increase in the value of J_{sc} in favor of the cell with the N719-*tpbe*-N719-TiO₂ film, relative to the J_{sc} value of the cell with the N719-TiO₂ film, considering the fact that the increase in the amount of the sensitizer is approximately 64% in favor of the N719-*tpbe*-N719-TiO₂ film relative to the amount of sensitizer in the N719-TiO₂ film.

In addition to the energy transfer represented by the reaction (3), the linked N719 can regenerate the oxidized, immobilized N719 according to the following reaction:



The regeneration of oxidized, immobilized N719 according to the reaction (4) is faster than that by I⁻ ions, due to the accepted slower movement of I⁻ ions in the electrolyte compared with electron transfer in the reaction (4). This rapid regeneration of oxidized N719 can contribute to the increase in photocurrent.

A direct pathway for electron transfer between the linked dye and TiO₂ may come into question. Except in one case,⁸ such remote electron transfer has been mentioned as a "probability".^{10,13,30} In the exceptional case,⁸ the reason given for such a remote electron transfer to the semiconductor was the short cyanide bridge of the complex Re^I(dcb)-(CO)₃-(CN)-Ru^{II}(byp)₂(CN) and the *cis* geometry at the Re centre between the anchoring dcb and the bridging cyanide ligand. Such direct electron injection or remote electron transfer from the excited, linked N719 to the conduction band of TiO₂ may be insignificant in our case, because the linker *tpbe* is rigid and does not allow rotation of the linked dye around *tpbe*, and the molecular layer of the immobilized dye would shield the linked dye from the TiO₂ surface.

The linkage of N3 to the immobilized N719 facilitated an approximately 10.5% increase in J_{sc} and the linkage of N749 to the immobilized N719 led to an approximate 7.6% decrease in J_{sc} , both values being calculated with reference to the J_{sc} obtained with N719 only (Table 1). The energy level diagram shown in Fig. 6 can explain these J_{sc} behaviors. As the LUMO levels of the immobilized and linked N719 are the same at -0.85 V, the charge and energy transfers from the linked N719 to the immobilized N719 are energetically favorable and a 36% increase in J_{sc} was achieved using this dinuclear complex. On the other hand, in the case of N749-*tpbe*-N719-TiO₂ (entry 5 in Table 1), the LUMO of N749 lies at a level lower (by as much as 0.19 eV (at -0.66 V)) than the LUMO of N719.^{3,24,31} Due to this unfavorable mismatch of the energy levels, the N749 dye molecules, which were excited to lower

Table 1 Photovoltaic parameters of the dye-sensitized solar cells, each with a Ru(II) sensitizer on its TiO₂ film^{a,b}

Sensitizer-TiO ₂	$J_{sc}/\text{mA cm}^{-2}$	V_{oc}/V	FF	η (%)
N719-TiO ₂	10.5	0.70	0.68	5.0
N749-TiO ₂	8.7	0.60	0.61	3.2
N3- <i>tpbe</i> -N719-TiO ₂	11.6	0.67	0.60	4.7
N719- <i>tpbe</i> -N719-TiO ₂	14.3	0.65	0.62	5.8
N749- <i>tpbe</i> -N719-TiO ₂	9.7	0.65	0.65	4.1
N719- <i>tpbe</i> -N749-TiO ₂	11.3	0.63	0.60	4.3
N3-TiO ₂	10.0	0.66	0.68	4.5
N3- <i>tpbe</i> -N3-TiO ₂	11.1	0.64	0.68	4.8
N719- <i>tpbe</i> -N3-TiO ₂	11.6	0.63	0.68	5.0
N749- <i>tpbe</i> -N3-TiO ₂	9.1	0.64	0.65	3.8

^a Each electrolyte consisted of 0.05 M I₂, 0.1 M LiI, 0.6 M 1,2-dimethyl-3-hexylimidazolium iodide, and 0.5 M 4-*tert*-butylpyridine in 3-methoxypropionitrile. ^b Measured under an illumination of 100 mW cm⁻².

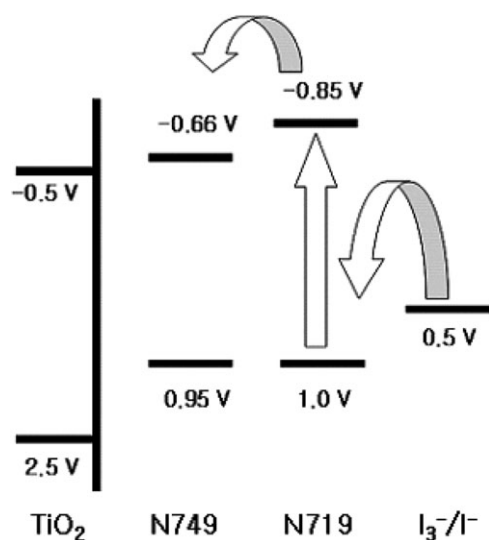


Fig. 6 Energy level diagram for TiO₂, N749, N719, and I₃⁻/I⁻, illustrating smooth electron transfer from a linked N719 to an immobilized N749.

levels than the LUMO of N719, can not transfer energy efficiently to the immobilized N719. Furthermore, even the higher excited states of N749 above the LUMO level of N719 may not necessary contribute to the increase in the J_{sc} , because the energy transfer from these states to N719 needs to compete with the vibrational relaxation within N749.

When N749 was immobilized onto TiO₂ and linked to N719, *i.e.*, the relative positions of the linked and immobilized sensitizers were switched, a rather smooth charge and energy transfers from the excited N719 to the immobilized N749 were expected as indicated by the following reaction.



This was indeed observed, as shown by entry 6 in Table 1; the J_{sc} is 11.3 mA cm⁻² which is larger than the J_{sc} shown in entry 5 (9.7 mA cm⁻²) obtained with a reversed combination of the same sensitizers. The J_{sc} of 11.3 mA cm⁻² amounts to a 7.6% increase compared with the J_{sc} of the DSSC with N719 only (entry 1).

The J_{sc} of the DSSC with the linked N3 (entry 3) is enhanced by only 10.5%, and that of the cell with the linked N719 (entry 4) by 36%, compared with the J_{sc} of the DSSC with N719. This observation is surprising considering the fact that the LUMO level of N3 is only slightly lower than that of N719.¹ This can be explained by the fact that N3, which is excited below the LUMO level of N719, is not expected to efficiently transfer electrons or energy to the immobilized N719, due to the differentiating energy barrier of N719 and consequent loss of incident light intensity. Furthermore, the N3 states that are energetically higher than the LUMO level of N719 may not necessary transfer their energy to N719 according to the reaction (3), because the energy transfer process competes with the vibrational relaxation within N3 as a result of collisions between the excited N3 molecules and solvent molecules. In addition to this, the molar absorptivities of N3 are lesser than those of N719 (Fig. 4a), favoring a higher J_{sc}

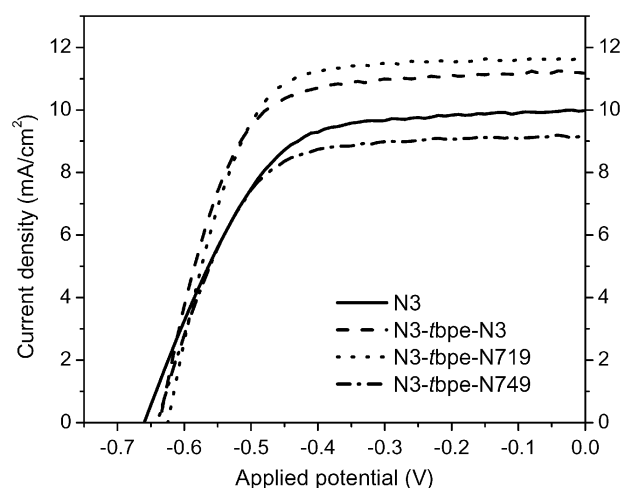


Fig. 7 J - V curves of the DSSCs prepared with films of N3-TiO₂ and Ru(II)-tbpe-N3-TiO₂, in which Ru(II) is N3, N719 or N749. The light intensity was 100 mW cm⁻².

for the DSSC with N719-tbpe-N719, compared with the J_{sc} of the cell with N3-tbpe-N719.

Similar results to the case of the N719-TiO₂ films were obtained with the N3-immobilized TiO₂ films (Fig. 7). Table 1 lists the corresponding photovoltaic parameters. Among the DSSCs with the immobilized N3, the DSSC with the N719-tbpe-N3-TiO₂ film showed the highest J_{sc} , while the DSSC with the N749-tbpe-N3-TiO₂ film showed the lowest. These results are consistent with the explanations provided above, *i.e.*, an energy barrier created between the immobilized and the linked dye reduces the charge and energy transfer from the linked dye to the immobilized dye. The charge transfer is found to be more efficient from N719 to N3 than that from N3 to N3, which suggests that a small but higher LUMO level of the linked dye is essential to achieve efficient transfer of the excited energy, by overcoming the loss due to competitive vibrational relaxation.

Other photovoltaic properties of DSSCs

Fig. 5 and Table 1 show that the V_{oc} s of the DSSCs with Ru(II)-tbpe-N719-TiO₂ are lower than the V_{oc} obtained with N719. One possible explanation for the decrease in V_{oc} due to the linkage of another dye to the immobilized dye might be a change in the flat band potential (V_{FB}) of TiO₂ in the DSSC.^{32,33} In the presence of a linked dye, such as N3 and N719, which contain carboxylic acid groups, the V_{FB} would shift positively due to the increased acidity on the TiO₂ film surface, which in turn results in a decrease in V_{oc} .³³ In the case of N749 purchased from Solaronix SA, the possible presence of a trace of acid in the product due to its synthetic procedure can also result in a positive shift in the V_{FB} and therefore in a decrease in V_{oc} .³ This explanation is consistent with the influence of the number of protons in N3 and its various protonated forms on the V_{oc} of DSSCs, *i.e.*, the V_{oc} decreases with increasing number of protons in the sensitizer.¹ Similar decreases in V_{oc} are noted due to the linkage of other Ru(II) dyes to the immobilized N3 in Fig. 7, albeit to a smaller extent,

compared with the decrease in V_{oc} in the case of the DSSCs with the immobilized N719.

Table 1 shows a general decrease in the FFs of the DSSCs with dinuclear complexes, compared with those of the cells with the mononuclear dyes, indicating a decrease in the conductivity of the I^-/I_3^- redox couple in the former case compared with that in the latter case. In contact with the additional layer of the dinuclear complex, the diffusion of both I^- and I_3^- ions are expected to slow down, leading to a general decrease in the conductivity of the electrolyte for the I^-/I_3^- redox couple. Fill factor results from a complex interplay of photocurrent generation and transport through the film, and is generally expected to depend on the mobility of the charge carriers in the film and electrolyte.^{34,35} The difference making moiety in the DSSC with dinuclear complex with respect to DSSC with mononuclear complex is the “attached dye”. The movement of I^- and I_3^- ions are expected to be hindered by this additional layer of the attached dye.

Due to the offsetting effects of the decreased V_{oc} and FF, the overall increase in the conversion efficiency (η) of the DSSC with the dinuclear complex N719-*tbpe*-N719 is marginal compared with the efficiency of its mononuclear variant (N719). Similarly, a lower V_{oc} offsets the increase in η of the DSSC with the dinuclear complex N719-*tbpe*-N3 compared with that of the DSSC with N3.

Therefore, the photovoltaic properties of DSSCs using the above discussed dinuclear Ru(II) complexes showed that these complexes can be used advantageously in DSSCs compared with the mononuclear Ru(II) complexes considering the LUMO levels. This study did not focus on optimizing the DSSC for higher efficiency, in view of the nature of this comparative study on the effects of a linkage of a Ru(II) dye to an immobilized Ru(II) dye on the photovoltaic parameters of the cell. The performance of the cell prepared using the TiO₂ film coated with the N719-*tbpe*-N719 can be further improved by using a scattering layer of large TiO₂ particles of approximately 400 nm,³⁶ by treating the TiO₂ surface with TiCl₄ before it is coated with the dye, as well as by covering the cell surface with an antireflection film.

Experimental

Linkage of Ru(II) to another TiO₂-attached Ru(II)

A typical linkage of Ru(II) dye to another TiO₂-attached Ru(II) dye was achieved in the case of N719 as follows. An N719-coated TiO₂ film of 13 μ m thickness (hereafter N719-TiO₂ film) was prepared on a 1.5 cm \times 1.5 cm-sized FTO glass plate (Libbey-Owens-Ford, TEC 8, 75% transmittance in the visible) using the Ti-Nanoxide TiO₂ paste (Solaronix SA), as described elsewhere.³⁷ 40.8 mg (0.224 mol) of *trans*-1,2-bis-(4-pyridyl)ethylene (*tbpe*, Aldrich) was dissolved in 100 mL of ethanol and the solution was sonicated under an Ar atmosphere. After 1 min, the N719-TiO₂ film was immersed in 30 mL of the *tbpe* ethanol solution, followed by refluxing for 4 h at approximately 75–80 °C under an Ar atmosphere.²⁴ The contents were allowed to cool to room temperature, and the *tbpe* bonded N719-TiO₂ film (*tbpe*-N719-TiO₂ film) was then washed with ethanol. This *tbpe*-N719-TiO₂ film was again

immersed in a 30 mL of a 0.5 mM N719 ethanol solution and heated at approximately 75–80 °C under reflux for 4 h in an Ar atmosphere. After cooling, the resulting N719-*tbpe*-N719-TiO₂ film was washed with ethanol, dried, and used to fabricate a DSSC.³⁷

The same procedure was used to synthesize the other dinuclear complexes using N719, N3 and N749 with various combinations (all purchased from Solaronix SA). The resulting complex in general is termed as Ru(II)-*tbpe*-Ru(II). Previously we attempted to synthesize Ru(II)-*tbpe*-Ru(II) by directly linking two Ru(II) dyes in ethanol solution using *tbpe*, *i.e.*, without employing a nanocrystalline TiO₂ film.¹⁵ This process led to the formation of an insoluble polymeric material that could not be used as a sensitizer. Owing to this previous experience we followed the route of linking the two Ru(II) dyes involving nanocrystalline TiO₂ film.

All chemicals were of analytical grade and used without further purification (99% pure, except *trans*-1,2-bis(4-pyridyl)ethylene which was 98% pure). All solutions were prepared using Milli Q (18.2 M Ω cm) H₂O. The assay was not available for N3, N719, and N749; they were purchased from Solaronix SA and used as obtained. The chemicals used for preparing DSSCs were purchased either from Solaronix SA or Aldrich, while KOH and C₂OH₆ were bought, respectively from Junsei and Carlo Erba.

Characterization of DSSCs

Unless otherwise specified, each TiO₂ film in the DSSCs had an active area of 0.4 cm \times 0.4 cm. The redox electrolyte solution consisted of 0.05 M I₂, 0.1 M LiI, 0.6 M 2,3-dimethyl-1-hexylimidazolium iodide, and 0.5 M 4-*tert*-butylpyridine in 3-methoxypropionitrile. An HP 8453A diode array spectrophotometer was used to obtain the UV-Vis absorption spectra of mononuclear and dinuclear sensitizers, both in solutions and on TiO₂ films. The photocurrent-voltage (J - V) curves were obtained over a potential range of -0.8 V to 0.2 V, using a Keithley M 236 source measure unit. A 300 W Xe arc lamp (Oriel), with an AM 1.5 solar simulating filter for spectral correction was used to illuminate the working electrode (from back side). The light intensity was adjusted to 100 mW cm⁻², using a Si solar cell.

Conclusion

The Ru(II) dye was linked through the *tbpe* linker to another TiO₂-immobilized Ru(II), using N3, N719 or N749 as the Ru(II) dye. Analyses of the absorption spectra of the synthesized dinuclear Ru(II)-*tbpe*-Ru(II) complex indicated that the amount of the linked dye was approximately 64% of that of the immobilized dye. Among the dinuclear dyes, the N719-*tbpe*-N719 dye showed the largest increase in J_{sc} (36%) for the pertinent DSSC compared with that of the cell with the immobilized N719 dye only. This enhancement is attributed to the high molar absorptivity of N719 and to the efficient intramolecular energy and charge transfer from the linked N719 to the immobilized N719 through the conjugated double bonds of *tbpe*. However, direct charge transfer from the linked dye to TiO₂ is not considered to be plausible under these experimental conditions, because the linked dye may be

shielded from the TiO₂ surface by a monolayer of immobilized dye and because of the rigid nature of *tbpe*. The energy and charge transfer from the linked dye to the immobilized one are found to be ineffective, if the LUMO level of the linked dye lies below that of the immobilized dye. The change in the flat band potential of TiO₂ due to the increased acidity as a result of the additional carboxylic acid groups of a linked dye is believed to be the reason for the lower V_{oc} of the DSSC with a dinuclear complex compared with that of the cell with a mononuclear dye.

Acknowledgements

This work was supported by the Korea Research Foundation Grant (KRF-2005-015-C00209) and the Sol-Gel Innovation Project.

References

- Md. K. Nazeeruddin, R. Humphry-Baker, P. Liska and M. Grätzel, *J. Phys. Chem. B*, 2003, **107**, 8981.
- Md. K. Nazeeruddin, A. Kay, I. Rodicio, R. Humphry-Baker, E. Miller, P. Liska, N. Vlachopoulos and M. Grätzel, *J. Am. Chem. Soc.*, 1993, **115**, 6382.
- Md. K. Nazeeruddin, P. Péchy, P. Renouard, S. M. Zakeeruddin, R. Humphry-Baker, P. Comte, P. Liska, L. Cevey, E. Costa, V. Shklover, L. Spiccia, G. B. Deacon, C. A. Bignozzi and M. Grätzel, *J. Am. Chem. Soc.*, 2001, **123**, 1613.
- Z.-S. Wang, H. Kawauchi, T. Kashima and H. Arakawa, *Coord. Chem. Rev.*, 2004, **248**, 1381.
- P. Wang, S. M. Zakeeruddin, J.-E. Moser and M. Grätzel, *J. Phys. Chem. B*, 2003, **107**, 13280.
- J.-J. Lagref, Md. K. Nazeeruddin and M. Grätzel, *Synth. Met.*, 2003, **138**, 333.
- A. S. Polo, M. K. Itokazu and N. Y. Murakami Iha, *Coord. Chem. Rev.*, 2004, **248**, 1343.
- R. Argazzi, C. A. Bignozzi, T. A. Heimer and G. J. Meyer, *Inorg. Chem.*, 1997, **36**, 2.
- C. J. Kleverlaan, M. T. Indelli, C. A. Bignozzi, L. Pavanin, F. Scandola, G. M. Hasselman and G. J. Meyer, *J. Am. Chem. Soc.*, 2000, **122**, 2840.
- C. Kleverlaan, M. Alebbi, R. Argazzi, C. A. Bignozzi, G. M. Hasselman and G. J. Meyer, *Inorg. Chem.*, 2000, **39**, 1342.
- A. Islam, F. A. Chowdhury, Y. Chiba, R. Komiya, N. Fuke, N. Ikeda and L. Han, *Chem. Lett.*, 2005, **34**, 344.
- K. Hara, M. Kurashige, S. Ito, A. Shinpo, S. Suga, K. Sayama and H. Arakawa, *Chem. Commun.*, 2003, 252.
- A. C. Lees, C. J. Kleverlaan, C. A. Bignozzi and J. G. Vos, *Inorg. Chem.*, 2001, **40**, 5343.
- R. Mosurkal, Y.-G. Kim, J. Kumar, L. Li, J. Walker and L. A. Samuelson, *J. Macromol. Sci., Pure Appl. Chem.*, 2003, **A40**, 1317.
- S.-R. Jang, R. Vittal, J. Lee, N. Jeong and K.-J. Kim, *Chem. Commun.*, 2006, 103.
- F. Loiseau, G. Marzanni, S. Quici, M. T. Indelli and S. Campagna, *Chem. Commun.*, 2003, 286.
- C. N. Fleming, K. A. Maxwell, J. M. DeSimone, T. J. Meyer and J. M. Papanikolas, *J. Am. Chem. Soc.*, 2001, **123**, 10336.
- V. Balzani, G. Bergamini, F. Marchioni and P. Ceroni, *Coord. Chem. Rev.*, 2006, **250**, 1254.
- L. De Cola, V. Balzani, F. Barigelli, L. Flamigni, P. Belser, A. von Zelewsky, M. Frank and F. Vögtle, *Inorg. Chem.*, 1993, **32**, 5228.
- M. Elvington and K. J. Brewer, *Inorg. Chem.*, 2006, **45**, 5242.
- P. Belser, R. Dux, M. Baak, L. De Cola and V. Balzani, *Angew. Chem., Int. Ed. Engl.*, 1995, **34**, 595.
- M. T. Indelli, M. Chiorboli, A. Prodi, C. Chiorboli, F. Scandola, N. D. McClenaghan, F. Puntoriero and S. Campagna, *Inorg. Chem.*, 2003, **42**, 5489.
- P. G. Potvin, P. U. Luyen and J. Bräckow, *J. Am. Chem. Soc.*, 2003, **125**, 4894.
- C. G. Garcia, N. Y. Murakami Iha, R. Argazzi and C. A. Bignozzi, *J. Photochem. Photobiol., A*, 1998, **115**, 239.
- B. J. Parsons, P. C. Beaumont, S. Navaratnam, W. D. Harrison, T. S. Akasheh and M. Othman, *Inorg. Chem.*, 1994, **33**, 157.
- Md. K. Nazeeruddin, F. De Angelis, S. Fantacci, A. Selloni, G. Viscardi, P. Liska, S. Ito, B. Takeru and M. Grätzel, *J. Am. Chem. Soc.*, 2005, **127**, 16835.
- R. J. Ellingson, J. B. Asbury, S. Ferrere, H. N. Ghosh, J. R. Sprague, T. Lian and A. J. Nozik, *J. Phys. Chem. B*, 1998, **102**, 6455.
- R. Memming, *Semiconductor Electrochemistry*, Wiley-VCH, Weinheim, 2001, ch. 10, p. 328.
- D. A. Skoog, F. J. Holler and T. A. Nieman, *Principles of Instrumental Analysis*, Saunders College Publ., 5th edn., 1998, ch. 15, p. 358.
- R. Argazzi, N. Y. Murakami Iha, H. Zabri, F. Odobel and C. A. Bignozzi, *Coord. Chem. Rev.*, 2004, **248**, 1299.
- A. Islam, H. Sugihara and H. Arakawa, *J. Photochem. Photobiol., A*, 2003, **158**, 131.
- Y. V. Pleskov and Y. Y. Gurevich, in *Semiconductor Photoelectrochemistry*, Translation ed. P. N. Bartlett, Consultant Bureau, New York, 1986, p. 241.
- T.-S. Kang, K.-H. Chun, J. S. Hong, S.-H. Moon and K.-J. Kim, *J. Electrochem. Soc.*, 2000, **147**, 3049.
- M. Svensson, F. Zhang, S. C. Veenstra, W. J. H. Verhees, J. C. Hummelen, J. M. Kroon, O. Inganäs and M. R. Andersson, *Adv. Mater.*, 2003, **15**, 988.
- T. A. Skotheim and O. Inganäs, *J. Electrochem. Soc.*, 1985, **132**, 2116.
- S. Hore, C. Vetter, R. Kern, H. Smit and A. Hinsch, *Sol. Energy Mater. Sol. Cells*, 2006, **90**, 1176.
- M. G. Kang, K. M. Kim, K. S. Ryu, S. H. Chang, N.-G. Park, J. S. Hong and K.-J. Kim, *J. Electrochem. Soc.*, 2004, **151**, E257.